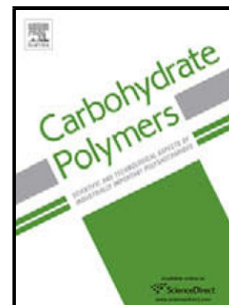


Journal Pre-proof

Sulfonated chitosan and phosphorylated chitosan coated polylactide membrane by polydopamine-assisting for the growth and osteogenic differentiation of MC3T3-E1s

Guijuan Han, Shuying Liu, Zhicheng Pan, Yucheng Lin, Shan Ding, Lihua Li, Binghong Luo, Yanpeng Jiao, Changren Zhou



PII: S0144-8617(19)31185-3
DOI: <https://doi.org/10.1016/j.carbpol.2019.115517>
Reference: CARP 115517

To appear in: *Carbohydrate Polymers*

Received Date: 30 April 2019
Revised Date: 17 October 2019
Accepted Date: 21 October 2019

Please cite this article as: Han G, Liu S, Pan Z, Lin Y, Ding S, Li L, Luo B, Jiao Y, Zhou C, Sulfonated chitosan and phosphorylated chitosan coated polylactide membrane by polydopamine-assisting for the growth and osteogenic differentiation of MC3T3-E1s, *Carbohydrate Polymers* (2019), doi: <https://doi.org/10.1016/j.carbpol.2019.115517>

This is a PDF file of an article that has undergone enhancements after acceptance, such as the addition of a cover page and metadata, and formatting for readability, but it is not yet the definitive version of record. This version will undergo additional copyediting, typesetting and review before it is published in its final form, but we are providing this version to give early visibility of the article. Please note that, during the production process, errors may be discovered which could affect the content, and all legal disclaimers that apply to the journal pertain.

© 2019 Published by Elsevier.

Sulfonated chitosan and phosphorylated chitosan coated poly lactide membrane by polydopamine-assisting for the growth and osteogenic differentiation of MC3T3-E1s

Guijuan Han, Shuying Liu, Zhicheng Pan, Yucheng Lin, Shan Ding*, Lihua Li, Binghong Luo, Yanpeng Jiao, Changren Zhou*

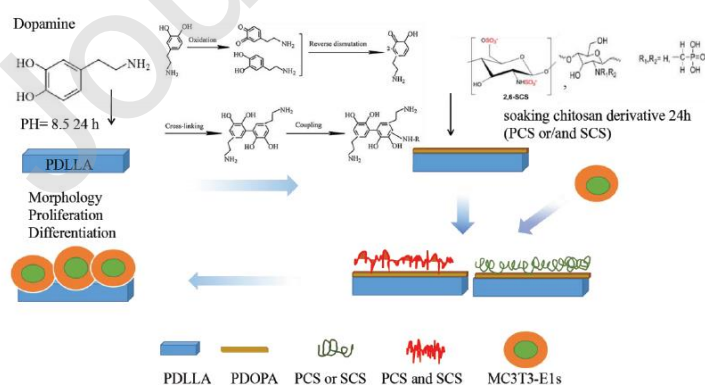
Department of Materials Science and Engineering, Jinan University, Guangzhou 510632, P. R. China

Engineering Research Centre of Artificial Organs & Materials, Jinan University, Guangzhou 510632, P. R. China

Corresponding Author

* E-mail address: tdingshan@jnu.edu.cn & tcrz9@jnu.edu.cn

Graphical Abstract



Highlights

- PCS and SCS, two chitosan derivatives with opposite charge were synthesized.
- Adhesion force and charge force were used to prepare composite membranes.
- The functional membranes showed excellent hydrophilicity and favored MC3T3-E1s proliferation and osteogenesis.

Abstract

In this study, a poly(D,L-lactide) (PDLLA) membrane was prepared by the solution casting method, then the surface of the membrane was modified by polydopamine (PDOPA) as a substrate, followed by adsorption of different chitosan derivative sulfonated chitosan (SCS) or/and phosphorylated chitosan (PCS) to obtain different functionalized membranes, and two kinds of chitosan derivatives characterized by FTIR, elemental analysis and zeta potential. And different membranes were evaluated through surface potential, hydrophilicity, surface morphology and chemical compositions. In vitro, the cell culture results showed that the membrane functionalized by chitosan derivative could promote the proliferation of MC3T3-E1s and enhance the osteogenic differentiation by up-regulating the expression level of osteogenic genes compared to the PDLLA and P₁/PDOPA membranes. Especially, when the outermost layer was SCS, the effect of promoting cell proliferation was better than that of PCS. However, for osteogenic differentiation, PCS had better quantitative experimental results than SCS. Therefore, SCS has superiority in promoting proliferation than PCS, but PCS is opposite in promoting osteogenic differentiation for MC3T3-E1s. The results suggested that PCS and SCS have the potential value to be used as a functional modified materials applied in bone tissue engineering.

Keywords: PDLLA; PDOPA; Modification; Sulfonated chitosan; Phosphorylated chitosan; Osteogenic differentiation

1. Introduction

Tissue engineering, an important emerging area in biomedical fields to create biological alternatives for harvested tissues and implants, has attracted wide attention in recent years. As one of the biomaterials with good biocompatibility, biodegradability, nontoxicity, excellent mechanical properties and processibility (Giannoudis, Dinopoulos, & Tsiridis, 2005; Rozalia Dimitriou, Elena Jones, Dennis McGonagle, & Giannoudis, 2011), polylactide (PLA) has been approved by Food and Drug Administration (FDA) of USA and widely utilized in biomedical fields such as bone tissue engineering, absorbable bone screws, surgical sutures and drug delivery device (Aruã C. da Silva, Michael J. Higgins, & Susana I. Córdoba de Torresi, 2019; Yuhao Deng et al., 2019). However, despite its advantages. Poly(D, L lactide) (PLLA) has insufficient biological activity and is far from meeting the strict requirements of bone regeneration. Besides, the hydrophobicity and poor osteogenic activity of PLLA also severely limit its application in bone tissue engineering field (Heqing Fu, Yin Wang, Weifeng Chen, & Xiao, 2015; Wenjun Liu et al., 2019).

Chitosan (CS), the deacetylated derivative of chitin, is a naturally occurring amino polysaccharide with favorable biological characteristics such as antibacterial activity, hemostasis, antitumor and healing the wound (Dimassi, Tabary, Chai, Blanchemain, & Martel, 2018). However, this natural polysaccharide exhibits a limitation in its reactivity and process ability because of a high density of hydrogen bonds between polymer chains in the solid state, and high viscosity due to the presence of intramolecular repulsive electrostatic forces that extend the polymer coil in solution (Wang & Liu, 2013). In literature, chemical modification, such as phosphorylation

(Shanmugam, Kathiresan, & Nayak, 2016), quaternization (Yizhuo Ren, Xin Zhao, Xiaofeng Liang, Peter X. Ma, & Baolin Guoa, 2017), carboxyalkylation (Wahid, Wang, Lu, Zhong, & Chu, 2017) and hydroxyalkylation (Shao et al., 2015), were utilized to produce new biofunctional materials in order to tailor the raw polymer properties.

It is reported that the sulfated CS (SCS) have been used as delivery systems for tissue repair and regeneration due to their capacity for binding to protein growth factors (Cao, Wang, Hou, Xing, & Liu, 2014; Cao, Werkmeister, et al., 2014), and showed to be the most efficient sulfated derivatives to direct neural differentiation (Doncel-Perez et al., 2018). In addition, SCS stimulated the proliferation of both human primary osteoblasts (OB) and the OB like stromal cell component of the giant cell tumor of bone (GCTB) at a concentration of $100 \mu\text{g.mL}^{-1}$, while it inhibited it at higher concentration ($1000 \mu\text{g.mL}^{-1}$) (T. Tang et al., 2011). Thus, sulfated CS could be used as bone repair biomaterials with the dual properties of bone induction and bone tumor inhibition. For the development of a new fibrous tissue, it is important that neovascularization occurs at the site of bone defect. It was proven by Yu et al. that 2,6SCS could promote revascularization for tissue regeneration and thus could be used as promising angiogenic biomaterial (Yu et al., 2018). Phosphorylated CS (PCS) exhibits much better hydrophilicity, solubility, protein adsorption and mineralization than unmodified chitosan (Pallab Datta, Dhara, & Chatterjee, 2012; P. Datta et al., 2013). Meanwhile, in comparison to CS scaffold, the PCS scaffold significantly enhances the *in vitro* osteogenic differentiation, indicated by the higher alkaline phosphatase (ALP) activity, denser mineralization deposition (Liu et al., 2018). Thus, it is helpful to immobilize SCS or/and PCS on PLLA material surface effectively to best take advantage of its bone regeneration ability.

Dopamine (DOPA), a critical functional element in mussel adhesive protein, can create a stable polydopamine (PDOPA) adherent layer on all kinds of substrates via oxidative self-polymerization (Lee et al., 2012). According to the literature (Haeshin, Dellatore, Miller, & Phillip B. Messersmith, 2007), the PDOPA layer can bind fibers

together to increase the strength of fibrous membrane. On the surface of materials, DOPA can form a thin PDOPA film in alkaline solution, which displays potential reactivity toward amine and thiol groups. So far, there have been a lot of relevant reports. Li, et al., utilized PDOPA as a spacer to immobilize bovine serum albumin (BSA) into porous polyethylene membranes (Nae Gyune Rim et al., 2012). Poh et al., studied the effect of Vascular endothelial growth factor (VEGF) functionalization of titanium by PDOPA coating on endothelial cells in vitro (Hua Liu , Wenling Li, Binghong Luo, Chen, & Zhou, 2017). Besides, our research group previously reported that surface functionalization of PLA membrane with chitooligosaccharide based on PDOPA coating can enhance the growth and osteogenic differentiation of MC3T3-E1 cells (Li et al., 2016) .

Inspired by previous studies, this study mainly aimed at surface modification of Poly(D,L-lactide) (PDLLA) with SCS or/and PCS to endow the material with positive effects on osteogenesis. For this purpose, SCS or/and PCS were designed to be immobilized onto PDLLA membrane surface via a facile approach based on the intermediate layer of PDOPA. Then, the effects of PDOPA coating and SCS or/and PCS immobilization on PDLLA membranes surface chemical composition, morphology, hydrophilicity and surface energy were studied in detail. Cell behaviors of the mouse embryo osteoblast precursor (MC3T3-E1) cells on different membranes surface were studied in terms of the proliferation, alkaline phosphatase activity, calcium deposition and gene expression level.

2. Materials and methods

2.1. Materials and reagents

Chitosan (Mw = 200 kDa), the degree of deacetylation was 80%, and was purchased from Golden-Shell Pharmaceutical Co. Ltd., Zhejiang, China and used without further dialyzed. Poly(D, L-lactide) (PDLLA, Mw = 150,000) was obtained

from Jinan Daigang Biological Engineering Co. Ltd and used as received. Tris(hydroxymethyl) aminomethane (Tris) and 3,4-dihydroxyphenethylamine (dopamine, DOPA) were purchased from Sigma-Aldrich and used as received. Cell test kit mainly include CCK-8 (Cell Counting Kit-8, Dojindo, Japan), ALP assays kit (Jiancheng Biotech, Nanjing, China), BCA protein assay kit (KeyGEN Biotech, Nanjing, China), Rhodamine phalloidin (Molecular Probes, USA) and 4,6-diamidino-2-phenylindole (DAPI, Molecular Probes, USA). All other reagents were of analytical grade and used without further purification.

2.2. Synthesis of the PCS and SCS

In this paper, Sulfonated chitosan (SCS), specifically referred to 2-N, 6-O-Sulfated chitosan (2,6-SCS) was synthesized according to the similar method as reported before (Rong Xing, 2005). In brief, 1.5 g CS was dissolved in 60 mL DMF and 1.2 mL dichloroacetic acid (DCAA) under stirring overnight. 5 mL HClSO_3 was added dropwise slowly to 20 mL DMF at 0 - 4 °C, which was then warmed to room temperature and added to the CS solution under magnetic stirring and N_2 atmosphere. The reaction was maintained at 60 °C for 2 h. Afterwards, 100 mL deionized water was added, and pH was adjusted to neutral with 2 M NaOH. Following, EtOH was added to precipitate the products, and the precipitation was washed with EtOH for 3 time, then was dissolved in water and dialyzed against water for 3 d with an 8000 Da Mw cut-off dialysis membrane. Consequently, 2,6-SCS was obtained by lyophilization.

Phosphorylated chitosan (PCS) was prepared according to a similar procedure reported elsewhere (A., N.M., V.M., & E., 2001; Yu Ji Yin, 2004). Briefly, CS solution was prepared by dissolving 2 g of CS powder into 100 g of 1 wt. % HAc solution. Phosphoric acid aqueous solution was added dropwise to the CS solution under stirring for 1 h. Then the temperature was raised to the designated temperature 70 °C and formaldehyde aqueous solution was incorporated drop-wise over 1 h with reflux. Heating was protracted for 8 h at the same temperature. The product was dialyzed

against distilled water for 72 h and freeze-dried for further use.

2.3. Preparation of modified PDLLA membranes

In brief, 0.5 g of PDLLA was dissolved to 20 mL chloroform solution under uniform stirring. After that the solution was cast on a petri dish at room temperature and let the solvent evaporate slowly. Then, PDLLA membrane was obtained by removing the residual solvent thoroughly in vacuum oven at 40 °C.

A certain amount of PDLLA membrane which has been ultrasonically cleaned with ethanol was immersed in Tris-HCl buffer solution (10.0 mM, pH 8.5) with 2.0 g/L of DOPA under magnetic stirring at room temperature for 24 h. Afterwards, the membrane was taken out and cleaned with ethanol and deionized water, and dried in a vacuum oven at 40 °C for 24 h. The PDOPA coated PDLLA membrane was named as P₁/PDOPA.

Additionally, the P₁/PDOPA membrane was further immersed into a 4.0 g/L SCS solution or PCS solution at room temperature for 24 h. Then the membrane was moved out and thoroughly rinsed with deionized water to remove unreacted PCS or SCS, with following drying in a vacuum oven at 40 °C for 24 h. The membranes were named as P₁/P₂/PCS and P₁/P₂/SCS, respectively.

To obtain double-layer modified membranes, the P₁/P₂/PCS and P₁/P₂/SCS were immersed in SCS and PCS solution, respectively, similar to the above procedures. The outmost layer of PCS or SCS were immobilized mainly by electrostatic interaction, and were named as P₁/P₂/P₃-S and P₁/P₂/S-P₃, respectively. The composition of the membranes was shown as Table. 1.

Table 1

Composition of PDLLA, P₁/PDOPA, P₁/P₂/PCS, P₁/P₂/SCS, P₁/P₂/P₃-S, P₁/P₂/S-P₃ membranes films.

Samples	PDLLA	PDOPA	PCS	SCS
PDLLA	√	/	/	/
P ₁ /PDOPA	√	√	/	/
P ₁ /P ₂ /PCS	√	√	√	/
P ₁ /P ₂ /SCS	√	√	/	√
P ₁ /P ₂ /P ₃ -S	√	√	①	②
P ₁ /P ₂ /S-P ₃	√	√	②	①

P₁, P₂ and P₃ represented PDLLA, PDOPA and PCS respectively. ① and ② they both represented the chitosan derivative on the surface, and the number represents the order of PCS and SCS.

2.4. Characterization of PCS and SCS

The chemical composition of PCS and SCS was analyzed by an Fourier transform infrared spectra (FTIR, Bruker EQUINOX 55 FTIR, Germany). Zeta potential was measured by Nanometer (Nanobrook Omni, USA). Element content was quantified by an elemental analyzer (Vario EL, Germany). And the degree of substitution (DS) was calculated according to percent.

2.5. Characterization of modified membranes

Attenuated total reflectance-Fourier transformation infrared (ATR-FTIR, Bruker EQUINOX 55 FTIR, Germany) spectroscopy was utilized to analyze the surface compositions of the original and modified PDLLA membranes. The spectra was measured in a wavenumber range of 3500-500 cm⁻¹. The surface chemical compositions of the membranes were further analyzed by an X-ray photoelectron spectroscopy (XPS, Thermo ESCALAB-250 System, Australia) with an aluminum (mono) K α source (1486.6 eV). The aluminum (mono) K α source was operated at 15 kV and 150 W. For all the samples, the whole scan spectrum of all the elements of a high-resolution survey (pass energy = 20 eV) was performed. The binding energy of

C_{1s} (284.8 eV) was used as a reference.

Field emission scanning electron microscopy (FESEM, XL30 FESEM FEG, PHILIPS) was used to characterize the surface morphologies of the membranes. The root mean square (RMS) of different membrane materials was used to estimate the surface roughness by atomic force microscope (AFM, IX51, Olympus) image based on 5.0 $\mu\text{m} \times 5.0 \mu\text{m}$ scan area.

Furthermore, the surface static contact angle of the different membranes was measured by contact angle meter (Drop Shape Analysis System, KRÜSS, Germany) to characterize materials wettability and surface energy (SE).

And surface electric intensity of all films was measured by solid surface potential instrument (Surpass 3, Austria).

2.6. Cell culture

Mouse embryo osteoblast precursor (MC3T3-E1) cells were cultured in α -minimum essential medium (α -MEM, Gibco) supplemented with 10% fetal bovine serum (FBS, Gibco) and antibiotics (penicillin 100 U/mL, streptomycin 100 $\mu\text{g/mL}$, Sigma) in 5% CO₂ atmosphere at 37 °C. The culture medium was changed every 2 days until the cells reached confluence. Then, cells were detached with 0.1% trypsin containing 0.02% EDTA (Gibco). Cells were rinsed and resuspended in the fresh α -MEM culture medium. A density of 1×10^4 cells/mL was obtained.

All the membranes samples were soaked in 75% alcohol overnight, and then UV-sterilized for 1h on each side. After membranes washing twice with sterile PBS, placed in a 24-well culture plate at a density of 1×10^4 cells/well in triplicate, in which cells were seeded and cultured for different periods. After 1, 4 and 7 days seeding, a series of relevant tests were operated.

2.7. Cell metabolic activity

Cell Counting Kit-8 (CCK-8) assays were used to measure the metabolic activity of

MC3T3-E1s that were cultured on membrane samples for 1, 4 and 7 days according to the manufacturers' instructions. The cell metabolic activity results were presented by optical density (OD) measured at 450 nm via an enzyme-linked immunosorbent assay plate reader (Multiskan MK3, Thermo electron corporation, USA). For each test, three repetitions were performed.

2.8. Alkaline phosphate (ALP) activity

ALP assays kit (Nanjing Jiancheng Bioengineering Institute, China) and bicinchoninic acid (BCA) protein assay kit (Nanjing KeyGEN Biotech. Co., Ltd.) were applied to ALP activity. After being cultured for 1, 4 and 7 days, respectively, membrane samples were washed with sterile PBS to remove any debris and ensure that only viable adherent cells were on the materials. Then, 0.1% Triton X-100 lysis buffer was added, and cracked in incubator for 30 to 40 min. According to the manufacturer's instruction, corresponding optical density (OD) at 520 and 562 nm were measured using an enzyme-linked immunosorbent assay plate reader. The qualitative analysis was performed according to the specification (Nanjing Jiancheng Bioengineering Institute, China). Briefly, MC3T3-E1s were dyed, then marked images were observed under a stereomicroscope (Carl Zeiss Microscopy GmbH 37081 Göttingen, Germany).

2.9. Cell morphologies and cytoskeleton organization

FESEM and confocal laser scanning microscopy (CLSM; Zeiss-LSM710; Carl Zeiss Jena, Germany) were employed to investigate the morphology and cytoskeleton organization of cells that adhered to different membrane surfaces after cultured for 1 day, respectively. For CLSM analyzing, the samples were washed twice with PBS, fixed with 3.7% formaldehyde solution in PBS for 10 min and then washed two or more times with PBS, subsequently permeabilized with 0.1% Triton X-100 in PBS for 3 to 5 min at room temperature. Non-specific binding was blocked with 3% BSA for 1 h. Then incubated with rhodamine phalloidin for 30 min and DAPI for 5 min in the

dark. Samples were rinsed several times with PBS. Finally, drain excess PBS buffer solution from the samples and mount for further CLSM observation.

In brief, samples were washed twice with sterilized PBS and then fixed with 4% paraformaldehyde for 30 min, followed dehydrated with an ascending series of ethanol at room temperature. The acquired samples were lyophilized and sputter-coated with gold for FESEM observation.

2.10. Calcium deposition assay

After cultured for 14 and 21 days, samples were washed with sterile PBS to remove any debris and ensure that only viable adherent cells were on the materials. Fixed with 4% paraformaldehyde for 15 min at room temperature, then the calcium deposition was stained with alizarin red (AR) solution for 30 min at 37 °C and examined by stereomicroscope. The stained cells were desorbed with 10% cetylpyridinium chloride (CPC) in PBS and the OD values were measured at 540 nm.

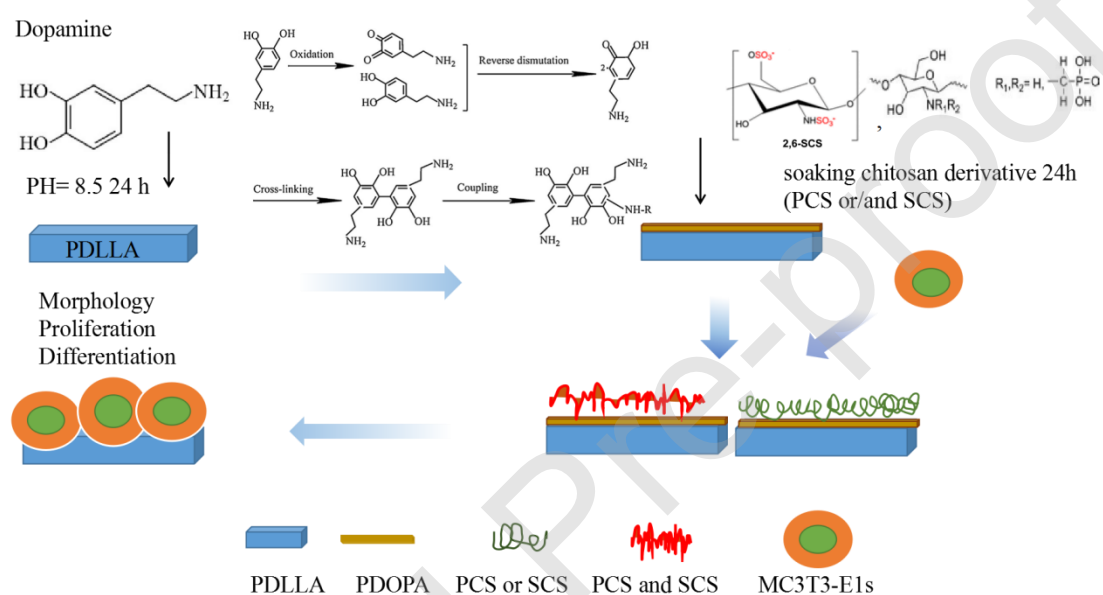
2.11. Quantitative Real-Time PCR assays

The gene expression was measured via real-time (RT) polymerase chain reaction (PCR) assay. MC3T3-E1 cells were seeded on each sample surfaces. After being cultured for 7 and 14 days, the total RNA from each samples was extracted using Trizol reagent (TaKaRa) according to the manufacturer's protocol and collected by ethanol precipitation. The amplifications were performed using the following protocol: 40 cycles of 95 °C for 15 s and 60 °C for 60 s. The genes included ALP, COL-I, Runx2 and OCN. To assess the target genes expression associated with osteogenic differentiation, RT-PCR was carried out using SYBR Green supermix. The $\Delta\Delta C_T$ method was used to calculate relative gene expression with β -actin as reference gene (housekeeping gene). All reactions were run in triplicate for three independent experiments.

2.12. Statistical analysis

All quantitative data were expressed as the mean \pm SD and were analyzed with Origin 8.5 (OriginLab Corp, Northampton, MA, USA). A value of $P < 0.05$ or $P < 0.01$ was considered statistically significant.

Entire process of the experiment is shown in Scheme 1 below



Scheme 1. The preparation route of the whole process of the experiment.

3. Results and discussion

3.1. Characterization of the PCS and SCS

To confirm the successful synthesis and provide basic parameters of the PCS and SCS, FTIR, zeta potential and elemental analysis were carried out, respectively. Changes in the functional groups after phosphorylation and sulfonation were characterized by FTIR spectroscopy. In Fig. 1A, the spectrum of CS depicted characteristic absorption bands at 3425, 2890, 1649 and 1580 cm^{-1} , which were assigned to $-\text{OH}$, $-\text{CH}_2$, $-\text{C}=\text{O}$ and $-\text{NH}_2$ stretching vibration respectively. The

presence of significant peak at 1649 cm^{-1} confirmed that CS was a partially deacetylated product. For PCS, the characteristic peak attributed to $-\text{NH}_2$ deformation has disappeared while a strong peak appeared at 1536 cm^{-1} , which might be assigned to the characteristics of amide II ($-\text{NH}-$). Meanwhile, the spectrum exhibited absorption bands at 902 cm^{-1} corresponding to the stretching vibration of P-O group (Yu Ji Yin, 2004). SCS has the best similarity with heparin and two novel absorption peaks appeared at 1224 cm^{-1} derived from $\text{O}=\text{S}=\text{O}$ asymmetrical vibration, and 795 cm^{-1} for C-O-S bond stretching, respectively (Zhou et al., 2009).

The detailed value of element percentage of CS as well as chitosan derivative used in later experiments were listed in Table 2. From the element analysis table, it may be inferred that PCS and SCS chitosan derivatives had been successfully synthesized after characteristic elements of P and S were detected. And the degree of substitution (DS) is given according to the following formula. (Mamuti, 2012).

$$X = \frac{M \cdot D_s}{162 + Y \cdot D_s}$$

X --- The percentage of characteristic element.

M --- Relative atomic mass of characteristic element.

Y --- The change in the relative molecular weight of a monomer.

162 --- Relative molecular weight of CS monomer.

In Fig. 1B, we could unambiguously discover the tendency that the zeta potential of both PCS and SCS used in this study were $35.5 \pm 1.5\text{ mv}$ and $-39.2 \pm 2.2\text{ mv}$ respectively. Charge difference also provided ideas for later multiple modifications.

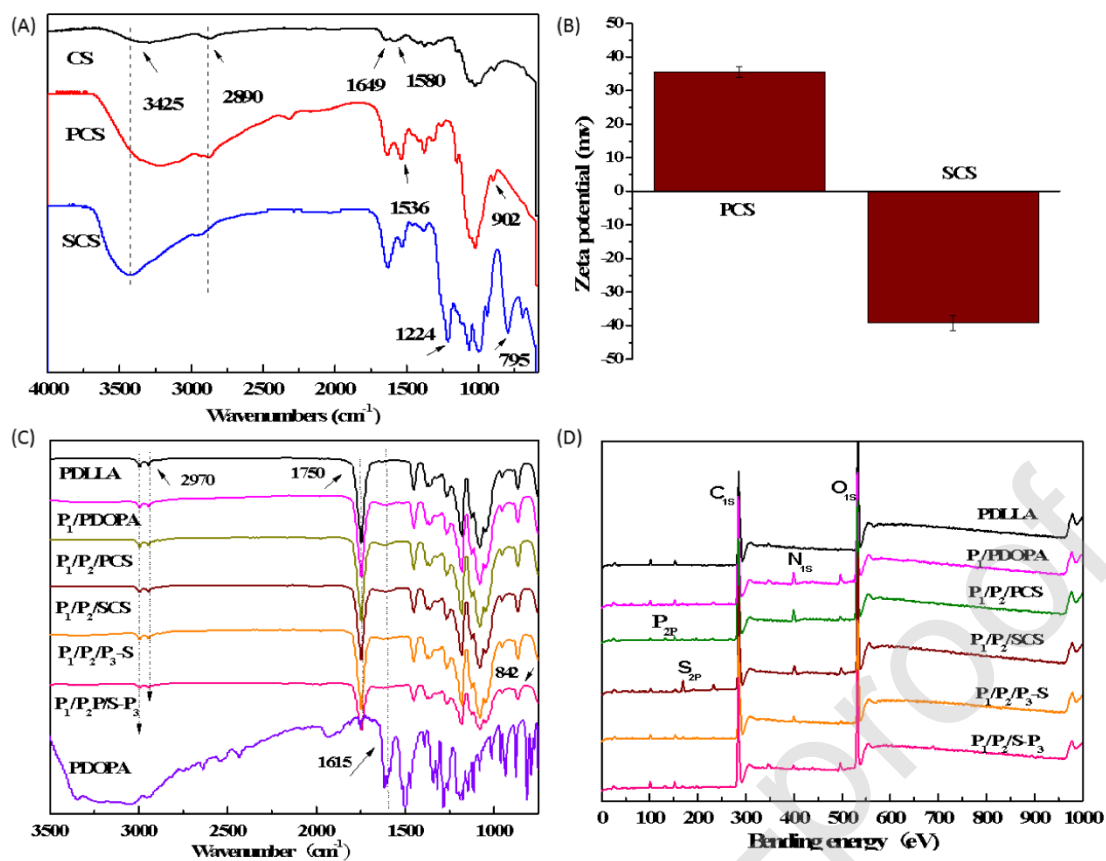


Fig. 1. ATR-FTIR spectra of CS, PCS, SCS (A), pure membrane and modified PDLLA membranes (C); Zeta potential of PCS, SCS with deionized water as a solvent (B); XPS spectra of pure membrane and modified PDLLA membranes (D)

Table 2

Surface elemental percentages of C, O, N, P, S, H of CS, PCS and SCS

Sample	C (%)	H (%)	N (%)	O (%)	P (%)	S (%)	DS
CS	37.40 ± 2.12	6.93 ± 0.24	6.67 ± 0.06	47.36 ± 3.12	0	0	-
PCS	27.15 ± 1.98	6.63 ± 0.41	4.92 ± 0.08	51.23 ± 2.78	5.99 ± 0.82	0	0.38 ± 0.01
SCS	20.39 ± 1.46	4.12 ± 0.18	3.99 ± 0.10	55.04 ± 1.86	0	12.56 ± 1.03	1.67 ± 0.02

DS: Degree substitution of materials.

3.2. Surface compositions of the membrane

The surface chemical structures of the original and modified membrane were analyzed by ATR-FTIR spectroscopy, and the result was shown in Fig. 1C. For pure PDLLA membrane, the strong peak around 1750 cm^{-1} was assigned to the stretching vibration of C-O, and peaks at 2957 cm^{-1} were attributed to C-H stretching vibrations of $-\text{CH}_3$ and $-\text{CH}-$. Compared to the pure PDLLA, some new absorption peak appeared after modified with PDOPA. The absorption peak at 1615 cm^{-1} was ascribed to the over-lap of C=C stretching vibration in aromatic ring and N-H bending vibration of PDOPA (Wufeng Yang, 2016). After surface modification with PCS or SCS, several characteristic absorption peaks were observed at 842 cm^{-1} and 1224 cm^{-1} , corresponding to the P-O stretching vibrations and O=S=O asymmetric vibration. The results suggested that PDOPA, PCS and SCS have been immobilized onto the PDLLA membrane surface, respectively. A few subtleties need to be explained here. According to literature reports (Wenjun Liu et al., 2019), dopamine owns excellent ability to adhere to nearly all kinds of substrates, and a thin PDA layer can be formed on the surface of the substrate via the oxidative selfpolymerization. Moreover, the PDA layer can be used as a secondary reaction platform to react with compounds containing nucleophilic groups such as amino, imino or sulfhydryl group by covalent and non-covalent interactions including Michael addition reaction, hydrogen and Van der Waals force. Therefore, the good stability of the PCS or SCS layer on the surface of the modified membranes may be reasonably attributed to the interactions between the amino, imino and hydroxyl groups of PDA and CS derivatives by the formation of covalent or noncovalent bonds.

The surface chemical compositions of the membrane materials were further analyzed by XPS, and the results were shown in Fig. 1D and Table 3. In Fig. 1D, the characteristic peaks of C_{1s} and O_{1s} can be observed for pure PDLLA, indicating the main surface composition of carbon and oxygen on the PLLA surface. Compared to original PDLLA membrane, new peaks were observed of N_{1s} at 400.16 eV appeared in the spectra of all modified membranes, which was ascribed to the nitrogen element

in the top layer of PDOPA and PCS and SCS. Besides, P_{2p} at 130.0 eV and S_{2p} at 168.2 eV were observed in the XPS spectra for $P_1/P_2/PCS$, $P_1/P_2/SCS$ composite membrane, respectively. However, since surface-attached PDOPA, PCS and SCS can be easily removed by ultrasonic washing with deionized water (Li et al., 2016). So, it can be concluded that PDOPA, PCS and SCS have been covalently immobilized on PDLLA membrane surface successfully. Furthermore, there was observed all element mentioned above for multiple-embellished membrane $P_1/P_2/P_3-S$ and $P_1/P_2/S-P_3$. These results indicate that PDOPA, PCS, and SCS were immobilized on the PDLLA membrane surfaces. It also can be proved by the content of N, P and S element (Table 3). N element content in the modification layer of $P_1/P_2/PCS$ membranes was 4.80%, and then decreased to 4.37%, 3.84%, 1.82% and 2.01% after further modification with PCS or/and SCS in $P_1/P_2/PCS$, $P_1/P_2/SCS$, $P_1/P_2/P_3-S$ and $P_1/P_2/S-P_3$ membranes, respectively. Since the molecular structural units of DOPA $(C_8H_9NO_2)_n$, PCS $(C_6H_{12}NO_4)_m(C_7H_{14}NPO_7)_n$ and SCS $(C_6H_{12}NO_4)_x(C_6H_{10}NS_2O_{10})_y$, the result can be reasonably expected since the percentage composition of N element in DOPA molecule was higher than that in PCS and SCS molecule. The content of P element in the $P_1/P_2/PCS$, $P_1/P_2/P_3-S$ and $P_1/P_2/S-P_3$ membranes surface was 0.76%, 0.49% and 0.43%, respectively. The values were lower in $P_1/P_2/P_3-S$ and $P_1/P_2/S-P_3$ membranes due to the second layer modification. The content of S element in $P_1/P_2/SCS$, $P_1/P_2/P_3-S$ and $P_1/P_2/S-P_3$ membranes was 2.85%, 0.49% and 2.13%, respectively. Similarly, the P element was partly covered by the outmost layer of SCS in $P_1/P_2/P_3-S$. Combining P and S element in the double-layer modified surface, we can summarize that the absorbed content in the inner layer exceeded the outer layer. This immobilization consequence is attributed to electrostatic interaction, group reaction and molecular specificity. But the absorption in inner layer is mainly attributed to the adhesion of PDOPA, and in the outer layer mainly due to the electrostatic adsorption between polymer with opposite charges.

Table 3

Surface elemental percentages of C, O, N, P, S of PDLLA, P₁/PDOPA, P₁/P₂/PCS, P₁/P₂/SCS, P₁/P₂/P₃-S, P₁/P₂/S-P₃ membranes films.

Samples	C1s (%)	O1s (%)	N1s (%)	P2p (%)	S2p (%)	O/C
PDLLA	70.11 ± 2.12	29.89 ± 0.89	0.00	0.00	0.00	42.60 ± 2.12%
P ₁ /PDOPA	68.12 ± 2.21	27.09 ± 0.92	4.80 ± 0.51	0.00	0.00	39.26 ± 1.65%
P ₁ /P ₂ /PCS	67.32 ± 3.52	27.55 ± 1.23	4.37 ± 1.00	0.76 ± 0.03	0.00	40.90 ± 1.87%
P ₁ /P ₂ /SCS	65.99 ± 3.48	27.32 ± 0.87	3.84 ± 0.36	0.00	2.85 ± 0.12	41.40 ± 2.01%
P ₁ /P ₂ /P ₃ -S	70.95 ± 4.82	25.86 ± 2.56	1.82 ± 0.42	0.49 ± 0.02	0.29 ± 0.04	36.44 ± 1.53%
P ₁ /P ₂ /S-P ₃	70.72 ± 4.32	26.38 ± 1.89	2.01 ± 0.23	0.43 ± 0.01	2.13 ± 0.08	37.30 ± 0.96%

The values were obtained by XPS.

3.3. Morphology and hydrophilicity of the membrane

FESEM was used to observe the surface morphologies of the membranes. The results were given in Fig. 2A. The original PDLLA membrane showed a smooth surface, while a rougher surface with a visibly convex layer was acquired for the P₁/PDOPA composite membrane due to PDOPA coating, leading to the embossment on the surface of the membrane. In addition, the fluctuation on the surface became weaker with further surface immobilization by single modified PCS or SCS. After immobilized by modified SCS and PCS, there were a lot of ups and downs on the membrane surface, and the surface roughness further increased to some extent.

The surface morphology of the unmodified membrane and modified membranes could be observed more visually in the two- and three-dimensional AFM micrographs

shown in Fig. 2B. The RMS value, as an indicator of surface roughness, was calculated accordingly. Higher RMS value means the rougher surface. The RMS values of PDLLA, P₁/PDOPA, P₁/P₂/PCS, P₁/P₂/SCS, P₁/P₂/P₃-S, P₁/P₂/S-P₃ membranes were 2.29 nm, 10.80 nm, 5.01 nm, 2.91 nm, 5.90 nm and 9.26 nm, respectively, which were supported by the SEM results. Both SEM and AFM results suggested that the surface modification with DOPA and modified PCS or/and SCS enabled the PDLLA membrane to have a rougher surface, which will be more favorable to cells adhesion and differentiation compared to the original PDLLA membrane. Because materials surface topography as well as surface roughness can influence cellular response (Groessner-Schreiber & Tuan, 1992; K. et al., 1996).

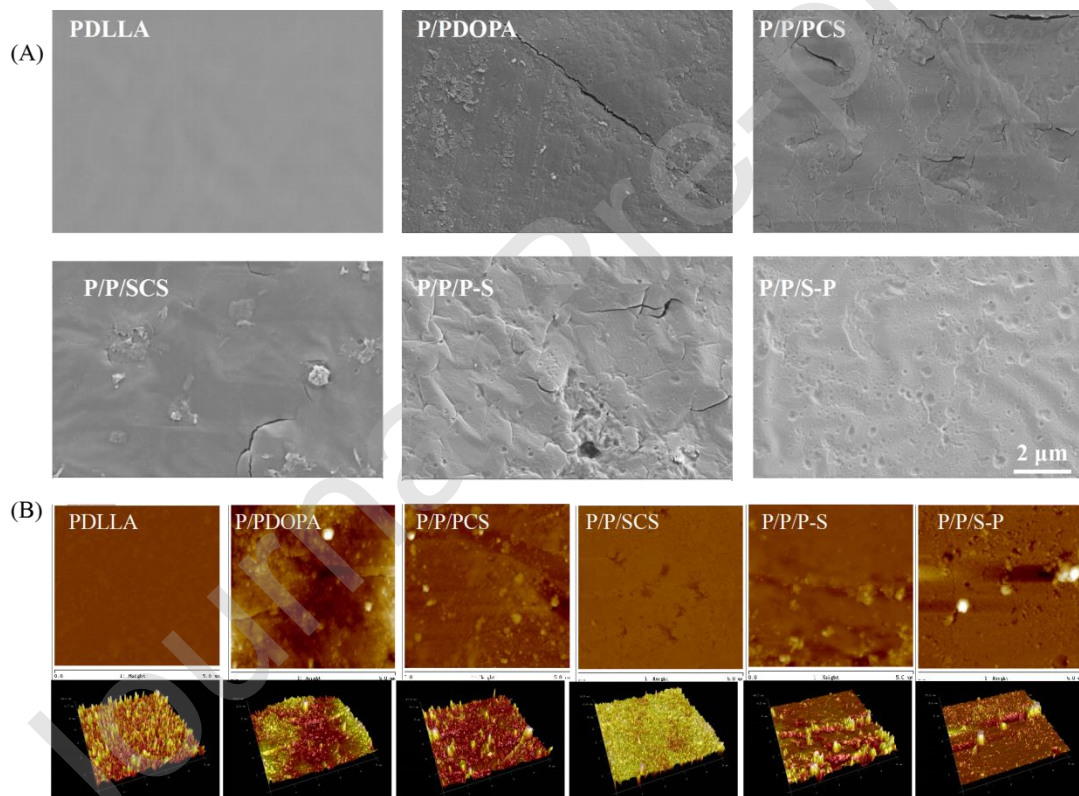


Fig. 2. FESEM (A); 2D and 3D AFM images of pure membranes and modified PDLLA membranes(B).

Surface hydrophilicity of the membranes is governed by both chemical composition and topographic structure (Jianhao Zhao et al., 2012). In this study, the contact angle (CA) values and surface energy (SE) of membranes were tested by using water and diiodomethane as the probe liquids. As is shown in Table 4, PDLLA membranes showed CA values of $87.6 \pm 0.02^\circ$ and $50.8 \pm 0.06^\circ$ against water and diiodomethane. After introducing PDOPA, PCS and SCS, the CA of the membranes declined firstly and then increased slightly, but still obviously lower than that of the original PDLLA membranes. The hydroxyl groups in the PDOPA molecular structure lead to the decrease of CA, while the sugar ring structure of PCS and SCS lead to the increase of CA slightly. Another reason may be the increasing in the roughness of membranes surface and the contact area with the droplets after surface modification by PDOPA, PCS and SCS.

The Owens-Wendt method is the most commonly used method for determination of SE. It has been shown that the Owens–Wendt method with a pair of nonpolar liquid and polar liquids gave minimum errors (D.K. & R.C., 1969; Jinhong Jiang, Liping Zhu, Lijing Zhu, Baoku Zhu, & Xu, 2011). SE, which mainly affected by the material surface composition and hydrophilicity, is often used to evaluate the surface adhesivity, wettability and biocompatibility, etc. The higher SE, the smaller contact angle and higher hydrophilicity of the membrane surface. In this research, SE of different membranes, and polar and disperse parts of SE were obtained according to the Owens–Wendt method, and the results are shown in Table 4. Here, γ_s refers to the total SE of the membranes, γ_s^p and γ_s^d represent the disperse and polar parts, respectively, γ_{s0} refers to the total surface energy of pristine PDLLA membranes, $(\gamma_s - \gamma_{s0})/\gamma_{s0}$ represents the changes in γ_s of the PDOPA and PCS or/and SCS modified PDLLA in comparison with that of the pristine PDLLA membrane. The SE of PDLLA membrane was 33.90 mN/m due to the weak interaction of Van der Waals force. But when coating with PDOPA, PCS or/and SCS layers, the SE of the membranes increased to 49.16, 43.31, 42.79, 41.85 and 38.64 mN/m, respectively. Moreover, the value of the polar component γ_s^p increased remarkably, but the dispersion component

γ_s^d changed very little, indicating the polar component plays the main role in contributions to the increase of the SE. The introduction of the PDOPA, PCS and SCS layers with abundant polar groups resulted in the strong hydrogen interaction between the molecules and the increase of the polar component γ_s^p value.

Table 4

Surface energy components of the PDLLA, P₁/PDOPA, P₁/P₂/PCS, P₁/P₂/SCS, P₁/P₂/P₃-S and P₁/P₂/S-P₃ membranes.

Samples	Contact angle (deg)		Surface energy (mN/m)			
	Water	Diiodomethane	γ_s^d	γ_s^p	γ_s	$(\gamma_s - \gamma_{s0}) / \gamma_{s0}$
PDLLA	87.6 ± 0.02	53.2 ± 0.72	31.18 ± 6.0	2.76 ± 0.9	33.90 ± 5.1	—
P ₁ /PDOPA	53.2 ± 0.72	47.0 ± 0.44	25.83 ± 3.0	23.30 ± 1.6	49.16 ± 4.6	0.45
P ₁ /P ₂ /PCS	66.7 ± 1.66	42.0 ± 0.22	31.38 ± 1.1	11.93 ± 2.3	43.31 ± 1.1	0.28
P ₁ /P ₂ /SCS	68.0 ± 0.10	42.2 ± 4.78	31.73 ± 1.3	11.06 ± 2.8	42.79 ± 1.5	0.26
P ₁ /P ₂ /P ₃ -S	70.8 ± 0.14	44.0 ± 0.30	28.14 ± 3.4	13.71 ± 4.5	41.85 ± 1.1	0.23
P ₁ /P ₂ /S-P ₃	71.4 ± 0.27	51.8 ± 0.65	27.08 ± 0.1	11.56 ± 1.0	38.64 ± 1.0	0.14

γ_s : Total surface energy; γ_s^p : Polarity component of surface energy; γ_s^d : Dispersion component of surface energy

3.4. Surface potential of membranes

Surface potential of the unmodified membrane and modified membrane was acquired by solid surface potentiometer. As shown in Fig. 3A, the average surface potential of PDLLA, P₁/PDOPA, P₁/P₂/PCS, P₁/P₂/SCS, P₁/P₂/P₃-S, P₁/P₂/S-P₃ were measured to be -35.04 ± 1.52 mv, -25.43 ± 0.30 mv, 7.64 ± 0.85 mv, -34.55 ± 0.25 mv, -35.93 ± 1.14 mv and -8.68 ± 0.25 mv, respectively. The result indicated that the amino of PDOPA increased the potential of pure PDLLA membrane. As is shown in Fig. 1A, PCS with positive charge increased the surface potential and (Yuefei Song, 2018) SCS with negative charge decreased the surface potential of the modified membrane, severally. Surface potential of biomaterials can dramatically influence cellular osteogenic differentiation (B. Tang et al., 2018). Uncharged surface, induce the weak osteogenic differentiation, overhigh surface potential, cause enhanced osteogenic differentiation and suitable surface potential, result in the strong osteogenic differentiation.

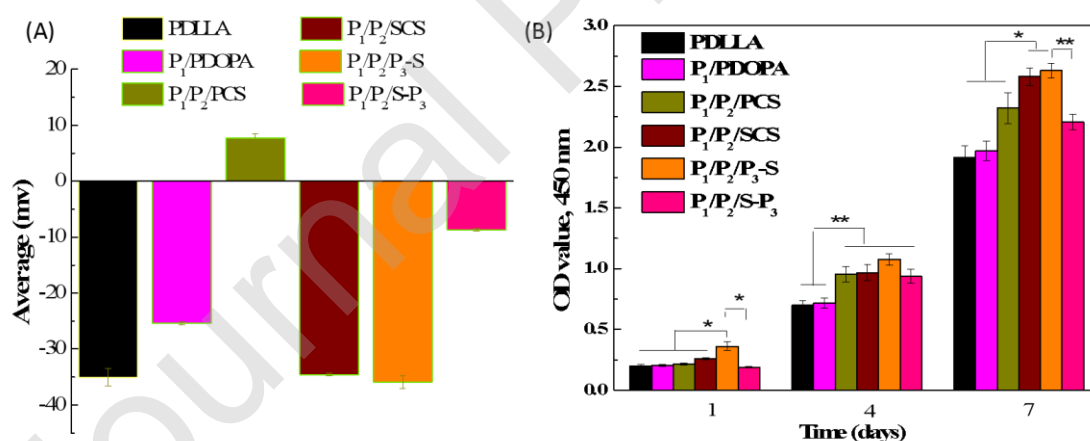


Fig. 3. Surface potential of pure membrane and composite membrane (A); Proliferation of MC3T3-E1 cells seeded on the PDLLA, composite membranes surfaces (B).

3.5. Cell metabolic activity

In the present study, the metabolic activity of MC3T3-E1 cells on different membrane surfaces was analyzed by CCK-8 assay, and the OD value of cells after 1, 4 and 7 days seeding on different membrane surfaces was obtained and displayed in Fig. 3B. It shows that the OD values of cells on all membrane surfaces generally increased with prolong culture time. However, notable differences could be detected between modified and unmodified PLLA membranes after 4 and 7 days seeding, especially in PSC or/and SCS modified membranes. Part of the reason could be that rough structures can promote cells proliferation (Azadeh Ghaee, 2017). The other reason may be the coated functional materials. The surface with hydroxyl and amine groups often exhibits good cytocompatibility, and is conducive to cells adhesion, spreading and proliferation (Altankov, Richau, & Groth, 2003; Becker et al., 2002). In addition, according to our research results, the modified layer with sulfonic acid group or/and phosphate radical group can better promote cell proliferation than that with hydroxyl and amine groups only. Furthermore, for the OD values of P₁/P₂/SCS and P₁/P₂/P₃-S, which film had SCS in the outlayer, had statistically significant difference from other groups. Surface potential of biomaterials can dramatically influence cellular proliferation (Altankov et al., 2003; Cai et al., 2006). But in this study, the value of different membranes surface zeta potential might be a critical parameter for cellular interactions, but the modified functional groups played an more important role in cell proliferation.

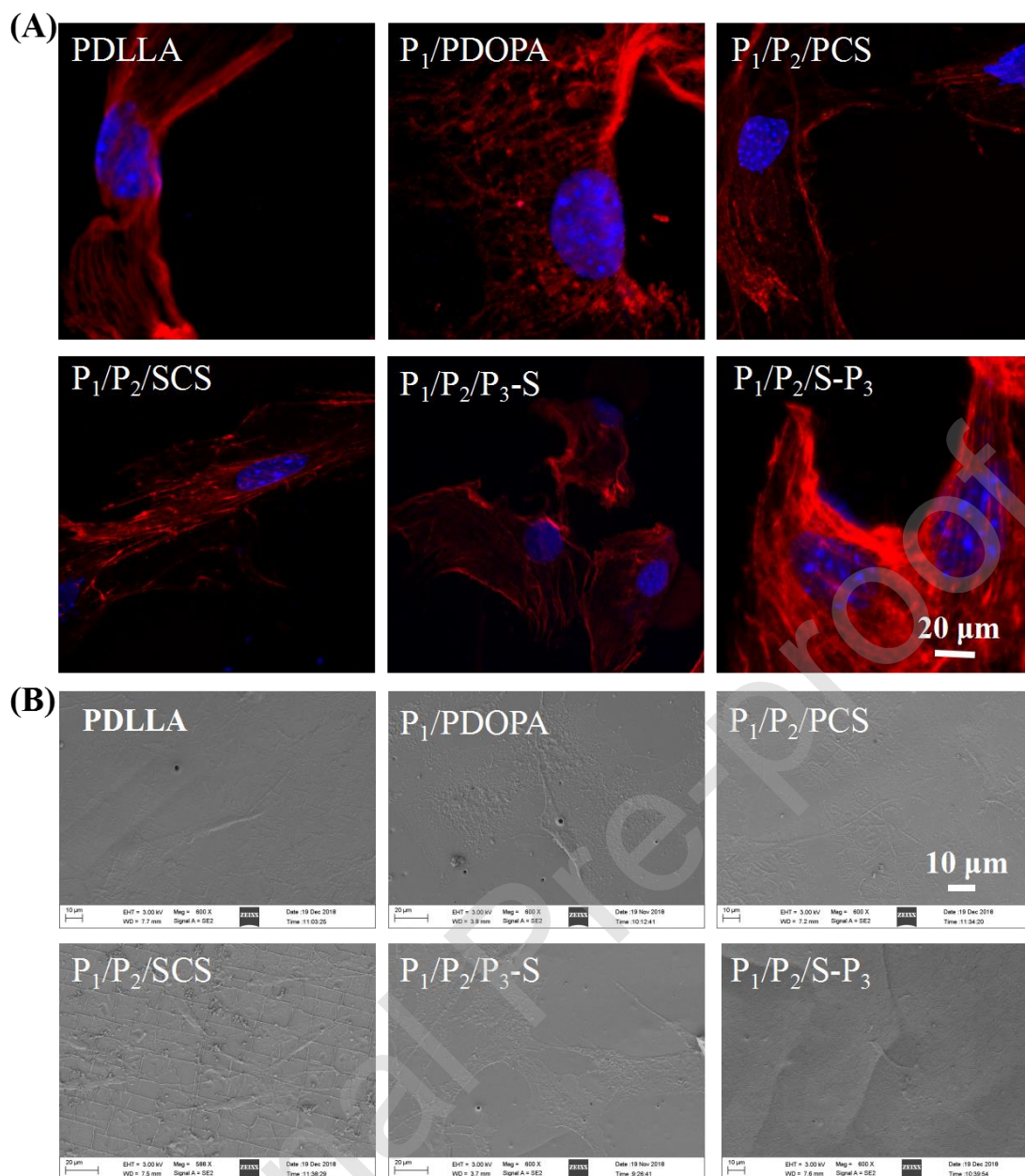


Fig. 4. CLSM (A) and FSEM (B) images of MC3T3-E1 cells on the materials surface after one day.

3.6. Cell morphologies and cytoskeleton organization

To gain a better understanding of the cellular response to the membranes, cell adhesion and spreading on membranes surface was studied. Cell cytoskeleton organization of MC3T3-E1s seeded on films by staining with Rhodamine phalloidin

for cytoskeleton and DAPI for nucleus, were further observed by CLSM (Fig. 4A). Cells on PDLLA surfaces tended to adopt an elongated morphology, unlike MC3T3-E1s on modified surfaces, which adopted bigger loose shape, especially those on the P₁/P₂/PCS, P₁/P₂/SCS membranes. Cell morphology, which is indirectly associated with cell viability, it can be included that PCS or SCS modified films energetic undergone general cell adhesion processes, such as substrate attachment, spreading and cytoskeleton development. FESEM micrographs of MC3T3-E1 cells after 1 day seeding on the different membranes were observed and presented in Fig. 4B. As expected, the spreading areas of MC3T3-E1 cells on modified membranes increased, especially in the groups of P₁/P₂/SCS and P₁/P₂/P₃-S membranes, which compared with others, owed more cells, suggesting that PCS, especially SCS modified substrates favored cell attachment and spreading.

3.7. ALP activity, ALP staining and calcium deposition

ALP is an early marker associated with osteoblast differentiation toward the osteocytic phenotype. And it was recognized as one of the key roles in the early stage of matrix mineralization (Becker et al., 2002). The quantitative analysis of ALP activities in MC3T3-E1 cells grown on the different PDLLA membranes after 1, 4 and 7 days seeding were measured and shown in Fig. 5A. The activities of all samples show a time-dependent pattern. At the beginning, there were no significant difference between the PCS or/and SCS modified PDLLA membranes groups, but P/P/PCS sample has a statistically significant difference ($P < 0.05$) to the PDLLA or P₁/PDOPA samples. At day 7, the ALP activities in each groups have similar tendency to that at day 4, but the difference became bigger between PCS or/and SCS modified films and PDLLA, P₁/PDOPA films, and there are statistical significant difference even between the P₁/PDOPA and PDLLA groups. Similar results were obtained by ALP qualitative detection as shown in Fig. 5C. The cell proliferation at day 7 on the P/P/SCS and P/P/P-S membrane surface is higher than on the other membranes surface (Fig. 3B),

but on the P₁/P₂/PCS and P₁/P₂/SCS samples, the ALP activity was higher than that on the other samples, especially on the P/P/PCS sample which was the highest (Fig. 5A). This indicates that when the outside layer is SCS, it is beneficial for MC3T3-E1s cell proliferation, but the outside layer of PCS benefits for ALP activity. In another word, PCS can promote the preosteoblast MC3T3-E1s to differentiate into osteoblasts.

In addition, calcium deposition, which is known to occur after ALP activation, was evaluated by alizarin red (AR) staining (Fig. 5B). Compared to PDLLA membrane, more mineralized nodules appeared on modified PDLLA membranes. Especially, more orange-red nodules were observed in the P/P/PCS and P/P/SCS groups compared to other groups. In addition, the results of quantification of AR staining dissolved in 10% CPC solution was shown in Fig. 5C, which further verified the conclusion mentioned above. Combined the result of ALP and AR staining together, it can be concluded that no matter which ingredient we introduced, coated PDOPA, SCS or/and PCS, especially the latter two, can increase the MC3T3-E1s osteogenic differentiation on PDLLA membranes. And for the modification with chitosan derivatives, PCS and SCS, the effect of single component modification is better than that of double component modification.

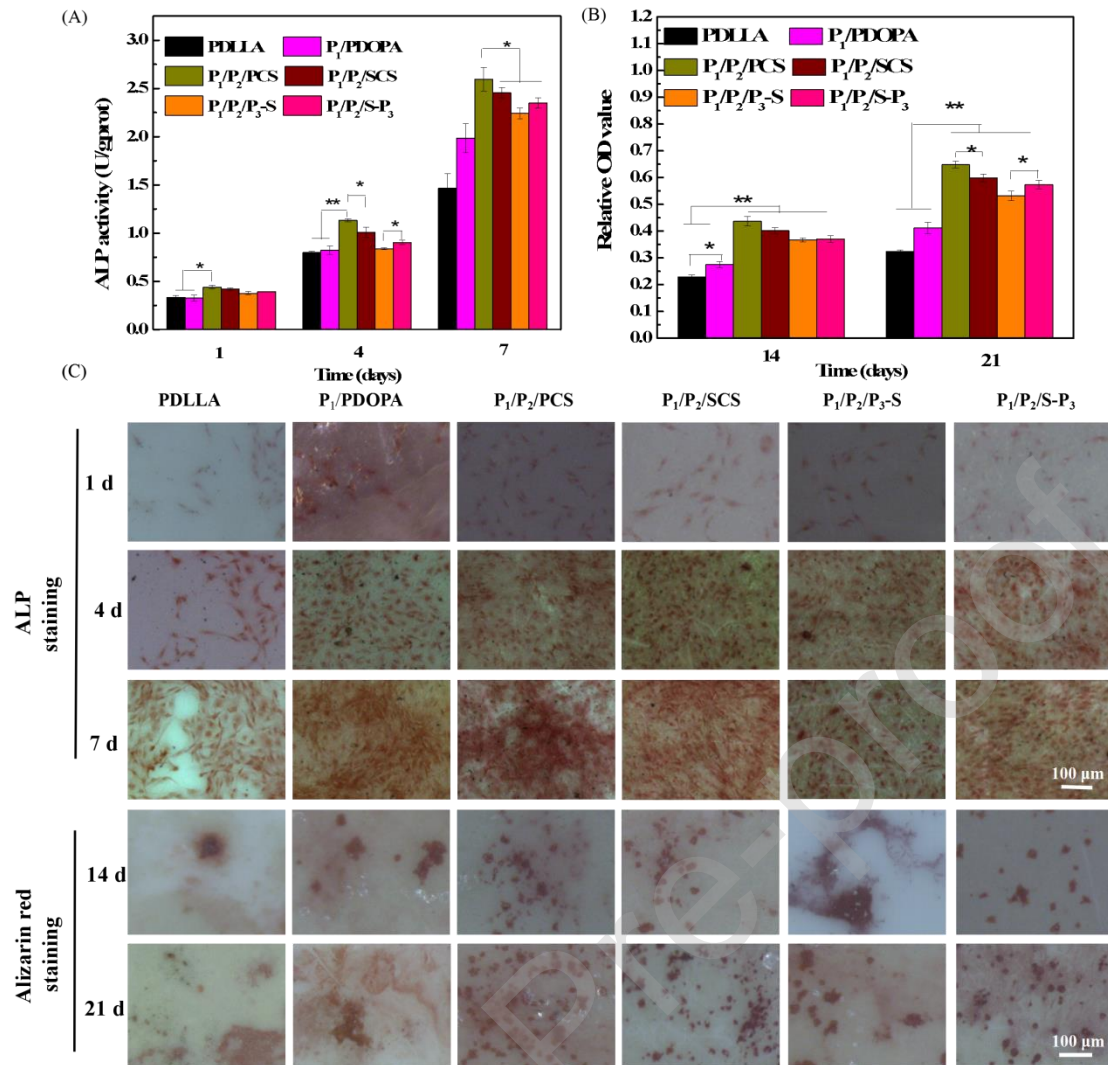


Fig. 5. ALP activities in MC3T3-E1 cells (A) and ALP staining (C) on day 1, 4 and 7, Alizarin red staining (C) and quantification of AR staining of cells on day 14, 21 (B).

3.8. Quantitative Real-Time PCR assays

In order to explore the differentiation effects of the membranes on MC3T3-E1 cells, the expression of osteogenesis related genes was evaluated by real-time PCR (Haishan Shi, 2019), as shown in Fig. 6. Generally, the expression levels of osteogenic markers (Runx2, ALP, Col-I and OCN) of MC3T3-E1s on PCS or/and SCS modified membrane were significantly up-regulated than that on PDLLA or

P/PDOPA membranes. Although on the day 14, the relative expression of Runx2 and COL-I were down-regulated compared with that on the day 7, the value of the PCS or/and SCS modified PDLLA membranes was higher than that on the PDLLA or P₁/PDOPA membranes (B. Tang et al., 2018). And in PCS or/and SCS modified groups, the effect of single component modification is better than double layer modification. In particular, when PCS was coated at the outer layer, the effect of functional materials up-regulated osteogenesis-related genes was better than that of SCS. In before, our research group had done similar work (Li et al., 2016). We prepared similar membranes (PDLLA/PDLLA-PDOPA/PDLLA-PDOPA-COS) and used them to enhance the growth and osteogenic differentiation of MC3T3-E1s. The morphology and hydrophilicity of the membrane were studied and the results of in vitro cell culture experiments revealed the PDOPA and COS layer especially the latter can significantly upregulate the ALP activity, and promote the osteogenic differentiation of MC3T3-E1 cells. All these seem to prove that surface functional group is more important for osteoblast differentiation than other related factors, such as surface zeta potential, surface roughness etc.

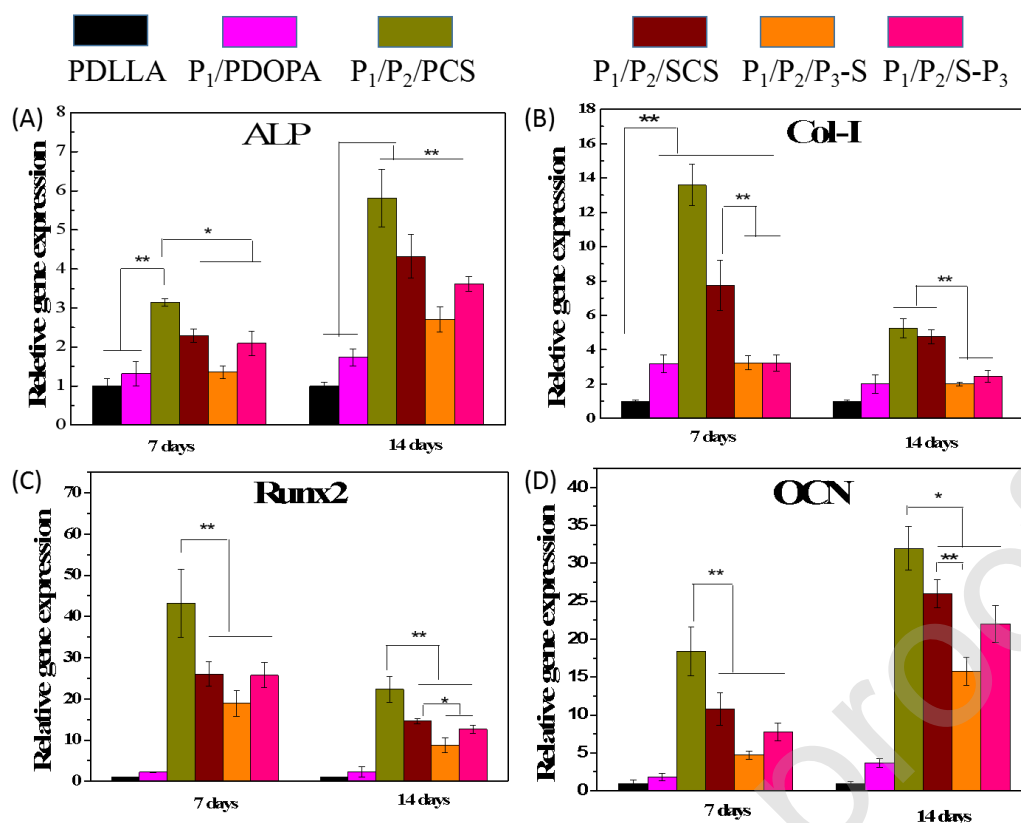


Fig. 6. The gene expressions of ALP (A), Col-I (B), Runx2 (C) and OCN of MC3T3-E1 cells on films.

4. Conclusion

In this work, we reported a series of functional PDLLA membranes modified by PCS or/and SCS by the intermediate of PDOPA layer for the growth and differentiation of MC3T3-E1s. These functional PDLLA membranes possess higher hydrophilicity than PDLLA membrane, and benefit the MC3T3-E1 cells adhesion, proliferation, alkaline phosphate activity and osteogenic differentiation. Specially, SCS has superiority in promoting MC3T3-E1s proliferation than PCS, but PCS has an advantage over SCS in promoting MC3T3-E1s osteogenic differentiation. In addition, the effects of single component of PCS or SCS are better than that of double component modification in the promotion of MC3T3-E1s proliferation and osteogenic differentiation. In summary, PCS and SCS can be expected to be practically used as

functional modified materials for bone tissue engineering, such as surface coating materials, 3D printing additive, hydrogel composition and so on.

Conflicts of interest

The authors declare no competing financial interest.

Acknowledgement

This work was supported by National Key R&D Program of China (Grant no. 2018YFC0311103) and the National Natural Science Foundation of China (31571030, 31570981 and 31400824).

References

- A., H., N.M., R. g., V.M., R., & E., A. (2001). N-methylene phosphonic chitosan: a novel soluble derivative. *Carbohydrate Polymers*, 44, 1-8.
- Altankov, G., Richau, K., & Groth, T. (2003). The role of surface zeta potential and substratum chemistry for regulation of dermal fibroblasts interaction. *Materialwissenschaft Und Werkstofftechnik*, 34(12), 1120-1128.
- Aruã C. da Silva, Michael J. Higgins, & Susana I. Córdoba de Torresi. (2019). The effect of nanoscale surface electrical properties of partially biodegradable PEDOT-co-PDLLA conducting polymers on protein adhesion investigated by atomic force microscopy. *Materials Science and Engineering: C*, 99, 468-478.
- Azadeh Ghaee, J. N., Parisa Danesh. (2017). Novel chitosan-sulfonated chitosan-polycaprolactone-calcium phosphate nanocomposite scaffold. *Carbohydr Polym*, 157, 695-703.
- Becker, D., Geißler, U., Hempel, U., Bierbaum, S., Scharnweber, D., Worch, H., & Wenzel, K. W. (2002). Proliferation and differentiation of rat calvarial osteoblasts on type I collagen-coated titanium alloy. *Journal of biomedical materials research*, 59(3), 516-527.
- Cai, K., Frant, M., Bossert, J., Hildebrand, G., Liefeth, K., & Jandt, K. D. (2006). Surface functionalized titanium thin films: Zeta-potential, protein adsorption and cell proliferation. *Colloids and Surfaces B-Biointerfaces*, 50(1), 1-8.
- Cao, L. Y., Wang, J., Hou, J., Xing, W. L., & Liu, C. S. (2014). Vascularization and bone regeneration in a critical sized defect using 2-N,6-O-sulfated chitosan nanoparticles incorporating BMP-2. *Biomaterials*, 35(2), 684-698.
- Cao, L. Y., Werkmeister, J. A., Wang, J., Glattauer, V., McLean, K. M., & Liu, C. S. (2014). Bone regeneration using photocrosslinked hydrogel incorporating rhBMP-2 loaded 2-N, 6-O-sulfated chitosan nanoparticles. *Biomaterials*, 35(9), 2730-2742.
- D.K., O., & R.C., W. (1969). Estimation of the surface free energy of polymers. *Journal of Applied Polymer Science*, 13, 1741-1747.
- Datta, P., Dhara, S., & Chatterjee, J. (2012). Hydrogels and electrospun nanofibrous scaffolds of N-methylene phosphonic chitosan as bioinspired osteoconductive materials for bone grafting. *Carbohydrate Polymers*, 87(2), 1354-1362.
- Datta, P., Ghosh, P., Ghosh, K., Maity, P., Samanta, S. K., Ghosh, S. K., . . . Dhara, S. (2013). In Vitro ALP and Osteocalcin Gene Expression Analysis and In Vivo Biocompatibility of N-Methylene Phosphonic Chitosan Nanofibers for Bone Regeneration. *Journal of Biomedical Nanotechnology*, 9(5), 870-879.

- Dimassi, S., Tabary, N., Chai, F., Blanchemain, N., & Martel, B. (2018). Sulfonated and sulfated chitosan derivatives for biomedical applications: A review. *Carbohydr Polym*, 202, 382-396.
- Doncel-Perez, E., Aranaz, I., Bastida, A., Revuelta, J., Camacho, C., Acosta, N., . . . Fernandez-Mayoralas, A. (2018). Synthesis, physicochemical characterization and biological evaluation of chitosan sulfate as heparan sulfate mimics. *Carbohydr Polym*, 196(15), 225-233.
- Giannoudis, P. V., Dinopoulos, H., & Tsiridis, E. (2005). Bone substitutes: an update. *Injury*, 36 Suppl 3, S20-S27.
- Groessner-Schreiber, B., & Tuan, R. S. (1992). Enhanced extracellular matrix production and mineralization by osteoblasts cultured on titanium surfaces in vitro. *Journal of Cell Science*, 101(1), 209-217.
- Haeshin, L., Dellatore, S. M., Miller, W. M., & Phillip B. Messersmith. (2007). Mussel-Inspired Surface Chemistry for Multifunctional Coatings. *Science*, 318, 426-430.
- Haishan Shi, X. Y., Fupo Hee, Jiandong Ye. (2019). Improving osteogenesis of calcium phosphate bone cement by incorporating with lysine: An in vitro study. *Colloids and Surfaces B: Biointerfaces*, 177, 462-469.
- Heqing Fu, Yin Wang, Weifeng Chen, & Xiao, J. (2015). Reinforcement of waterborne polyurethane with chitosan-modified halloysite nanotubes. *Applied Surface Science*, 346, 372-378.
- Hua Liu , Wenling Li, Binghong Luo, Chen, X., & Zhou, C. (2017). Icarin immobilized electrospinning poly(L-lactide) fibrous membranes via polydopamine adhesive coating with enhanced cytocompatibility and osteogenic activity. *Materials Science and Engineering C*, 79, 399-409.
- Jianhao Zhao, Wanqing Han, Mei Tu, Songwei Huan, Rong Zeng, Hao Wu, . . . Changren Zhou. (2012). Preparation and properties of biomimetic porous nanofibrous poly(L-lactide) scaffold with chitosan nanofiber network by a dual thermally induced phase separation technique. *Mater Sci Eng C Mater Biol Appl*, 32(6), 1496-1502.
- Jinhong Jiang, Liping Zhu, Lijing Zhu, Baoku Zhu, & Xu, Y. (2011). Surface Characteristics of a Self-Polymerized Dopamine Coating Deposited on Hydrophobic Polymer Films. *Langmuir*, 27, 14180–14187
- K., K., Z., S., Humrnert T, W., L., C. D., J., S., D., D. D., & D., B. B. (1996). Surface roughness modulates the local production of growth factors and cytokines by osteoblast-like MG-63 cells. *Journal of biomedical materials research*, 32, 55-63.
- Lee, Y. B., Shin, Y. M., Lee, J. H., Jun, I., Kang, J. K., Park, J. C., & Shin, H. (2012). Polydopamine-mediated immobilization of multiple bioactive molecules for the development of functional vascular graft materials. *Biomaterials*, 33(33), 8343-8352.

- Li, H., Luo, C., Luo, B., Wen, W., Wang, X., Ding, S., & Zhou, C. (2016). Enhancement of growth and osteogenic differentiation of MC3T3-E1 cells via facile surface functionalization of polylactide membrane with chitooligosaccharide based on polydopamine adhesive coating. *Applied Surface Science*, 360, 858-865.
- Liu, L., He, Y., Shi, X., Gao, H., Wang, Y., & Lin, Z. (2018). Phosphocreatine-modified chitosan porous scaffolds promote mineralization and osteogenesis in vitro and in vivo. *Applied Materials Today*, 12, 21-33.
- Mamuti, K. R. M. (2012). Performance of sulfonated cellulose based water-reducing agent for cement. *Concrete* (Vol. 10, pp. 74-76).
- Nae Gyune Rim, Seok Joo Kim, Young Min Shin, Indong Jun, Dong Woo Lim, Jung Hwan Park, & Shin, H. (2012). Mussel-inspired surface modification of poly(l-lactide) electrospun fibers for modulation of osteogenic differentiation of human mesenchymal stem cells. *Colloids and Surfaces B: Biointerfaces*, 91, 189-197.
- Rong Xing, S. L., Huahua Yu, Zhanyong Guo, Zhien Li, Pengcheng Li. (2005). Preparation of high-molecular weight and high-sulfate content chitosans and their potential antioxidant activity in vitro. *carbohydr Polym*, 148-154.
- Rozalia Dimitriou, Elena Jones, Dennis McGonagle, & Giannoudis, P. V. (2011). Bone regeneration: current concepts and future directions. *BMC Medicine*, 9(1), 1741-1751.
- Shanmugam, A., Kathiresan, K., & Nayak, L. (2016). Preparation, characterization and antibacterial activity of chitosan and phosphorylated chitosan from cuttlebone of *Sepia kobsiensis* (Hoyle, 1885). *Biotechnol Rep (Amst)*, 9, 25-30.
- Shao, K., Han, B., Gao, J., Song, F., Yang, Y., & Liu, W. (2015). Synthesis and characterization of a hydroxyethyl derivative of chitosan and evaluation of its biosafety. *Journal of Ocean University of China*, 14(4), 703-709.
- Tang, B., Zhang, B., Zhuang, J., Wang, Q., Dong, L., Cheng, K., & Weng, W. (2018). Surface potential-governed cellular osteogenic differentiation on ferroelectric polyvinylidene fluoride trifluoroethylene films. *Acta Biomater*, 74, 291-301.
- Tang, T., Zhang, G., Py Lau, C., Zheng, L. Z., Xie, X. H., Wang, X. L., . . . Kumta, S. M. (2011). Effect of water-soluble P-chitosan and S-chitosan on human primary osteoblasts and giant cell tumor of bone stromal cells. *Biomedical Materials*, 6(1), 015004.
- Wahid, F., Wang, H. S., Lu, Y. S., Zhong, C., & Chu, L. Q. (2017). Preparation, characterization and antibacterial applications of carboxymethyl chitosan/CuO nanocomposite hydrogels. *Int J Biol Macromol*, 101, 690-695.
- Wang, K., & Liu, Q. (2013). Adsorption of phosphorylated chitosan on mineral surfaces. *Colloids and Surfaces A: Physicochemical and Engineering Aspects*, 436, 656-663.

- Wenjun Liu, Ling Zhu, Yunfa Ma, Lihao Ai, Wei Wen, Changren Zhou, & Luo, B. (2019). Well-ordered chitin whiskers layer with high stability on the surface of poly(d,l-lactide) film for enhancing mechanical and osteogenic properties. *Carbohydrate Polymers*, 212, 277-288.
- Wufeng Yang, X. Z., Keke Wu, Xiaoyan Liu, Yanpeng Jiao, Changren Zhou. (2016). Improving cytoactive of endothelial cell by introducing fibronectin to the surface of poly L-Lactic acid fiber mats via dopamine. *Mater Sci Eng C Mater Biol Appl*, 69, 373-379.
- Yizhuo Ren, Xin Zhao, Xiaofeng Liang , Peter X. Ma, & Baolin Guoa. (2017). Injectable hydrogel based on quaternized chitosan, gelatin and dopamine as localized drug delivery system to treat Parkinson's disease. *International Journal of Biological Macromolecules*, 105, 1079-1087.
- Yu Ji Yin, X. Y. L., Jun Feng Cui, Chang Yong Wang, Xi Min Guo, Kang De Yao. (2004). A Study on Biomineralization Behavior of N- Methylene Phosphochitosan Scaffolds. *Macromolecular bioscience*, 4, 971-977.
- Yu, Y., Chen, R., Sun, Y., Pan, Y., Tang, W., Zhang, S., . . . Liu, C. (2018). Manipulation of VEGF-induced angiogenesis by 2-N, 6-O-sulfated chitosan. *Acta Biomaterialia*, 71, 510-521.
- Yuefei Song, Q. H., Tiemei Li, Yueke Sun, Xinxin Chen, Jing Fan. (2018). Fabrication and characterization of phosphorylated chitosan nanofiltrationmembranes with tunable surface charges and improved selectivities. *Chemical Engineering Journal*, 352, 163-172.
- Yuhao Deng, Aaron X. Sun, Kalon J. Overholt, Gary Z. Yu, Madalyn R. Fritch, Peter G. Alexander, . . . Hang Lin. (2019). Enhancing chondrogenesis and mechanical strength retention in physiologically relevant hydrogels with incorporation of hyaluronic acid and direct loading of TGF- β . *Acta Biomaterialia*, 83, 167-176.
- Zhou, H., Qian, J., Wang, J., Yao, W., Liu, C., Chen, J., & Cao, X. (2009). Enhanced bioactivity of bone morphogenetic protein-2 with low dose of 2-N, 6-O-sulfated chitosan in vitro and in vivo. *Biomaterials*, 30, 1715-1724.